# Electron beam characterisation

**Thomas Dutilleul, Joshua Priest, Bernd Baufeld**

*Electron beam welding (EBW) presents significant advantages in terms of welding performance when compared to other welding processes due to its small spot size, low divergence, high power density and low heat input. It is recognised in laser welding and cutting that reliable and reproducible results can only be achieved through the detailed understanding of the beam characteristics. The optical properties of the beam have long been neglected in EBW as the power output is often sufficient to achieve satisfactory results.*

*In recent years, it has been realised by industry that a similar approach should be applied to electron beam welding; therefore, companies such as aixACCT have developed methods of electron beam analysis with a high duty cycle that can be used in industrial environments.*

*The aixACCT electron beam analyser is capable of analysing beams at powers of up to 30 kW and was used to create a mapping of the electron beam, focal length, spot size and caustics over a wide range of powers.*

***Характеризиране на електронния лъч (Томас Дутилюл, Джошуа Приист, Бернд Бауфелд).*** *Електронолъчевото заваряване (ЕЛЗ) представя значителни предимства по отношение на производителността на заваряване в сравнение с други заваръчните процеси, поради малкия размер на мястото на въздействие на лъча (петно), ниско дивергенция, висока плътност на мощност и ниска топлинна мощност. Признато е при лазерно заваряване и рязане, че надеждни и възпроизводими резултати могат да бъдат постигнати само при подробно разбиране на характеристиките на лъча. Оптичните свойства на лъча отдавна са пренебрегвани при ЕЛЗ, като изходната мощност често е достатъчна, за да се постигне задоволителни резултати.*

*През последните години в индустрията се осъзнава, че подобен подход следва да се прилага за електронолъчевото заваряване; следователно, компании като aixACCT са разработили методи за анализ на електронен лъч с дълъг работен цикъл, който може да се използва в индустриални условия.*

*Електронолъчевият анализатор на aixACCT е в състояние да анализира лъчи с мощности до 30 kW и се използва за създаване на карта на електронния лъч, фокусното разстояние, размера на мястото на въздействие на лъча и плътността му в широк спектър от мощности на лъча.*

## Introduction

The usual electron beam welding parameters, beam current, lens current, working distance and travel speed did prove themselves insufficient to achieve identical welds on different machines. This transferability issue is inconvenient in a production environment where one machine may be used for the parameter development but another for production. Beam analysis aims to bring the missing parts that may make the transferability of parameters easier, that is the value of the beam position, diameter and divergence at the workpiece.

### *1.1. Electron beam guns*

Thermionic electron beam guns consist of an emitting source, often tungsten or LaB6, that is resistively heated to a high temperature by a strong current. This results in electron emission. These emitted electrons are then accelerated by a high potential towards the workpiece. This is the principle of the diode gun; the emitting source is called the cathode and the electrode yielding the potential is called the anode. The triode gun principle works the same as the diode gun but with the addition of another electrode between cathode and anode. This electrode is called the bias electrode but is also referred to as the grid, control electrode or even Wehnelt in literature [1]. Its function is to control the amount of electrons being emitted by the cathode, and thus control the

current output (Ib) in welding. Whilst doing this it also focuses the electrons into as narrow a point as possible called the crossover point. The crossover point is the point where the minimum beam diameter is attained and then starts to diverge again. Once diverging, the electron's ray appears as if formed by a virtual crossover [2].

### *1.2. Emittance*

The emittance or beam parameter product is the product of a beam's divergence half angle and its radius at the crossover. This value represents the quality of the beam with the smaller the number the higher the quality.

$$E = \frac{d}{2} * \frac{\alpha}{2} \quad (1)$$

With d the beam diameter at focus and α the divergence angle.

### *1.3. Magnetic lenses*

As the beam leaves the anode, it continues diverging and this causes the power density to decrease. Hence, the use of a magnetic lens called a condenser to refocus the beam onto the workpiece.

Magnetic lenses in their simplest form are a coil of conductive wire within an iron casing. Passing a current through this coil then creates a magnetic field, this current is referred to as the lens current ($I_L$) in welding.

The thin magnetic lens focal length can be generally written as [3]:

$$\frac{1}{F} = \left[\frac{e}{8mV_{nr}}\right]\int B_z^2 dz \quad (2)$$

With e and m being the charge and mass of the electron respectively, $V_{nr}$ being the accelerating potential and $B_z$ being the axial magnetic field in the lens.

$B_z$ is supposed constant and is directly proportional to the lens current so that equation (2) can easily be approximated by:

$$\frac{1}{F} = K\frac{I_L^2}{V_{nr}} \quad (3)$$

With K a constant that depends on the lens fabrication.

Due to the high accelerating voltage, the electrons going through the lens are so fast that they can be considered *relativistic*. Magnetic Lens formulas can be corrected by a factor [3]:

$$V_{nr} \to V\left[1+\frac{eV}{2mc^2}\right] = V(1+0.978*10^{-6}V) \quad (4)$$

This correction factor accounts for 6% for a 60 kV gun.

What is of particular interest here is that magnetic lenses behave exactly like optical lenses and obey the optical thin lens formulas. An object A produces an image B through a lens of focal length F as per:

$$\frac{1}{A}+\frac{1}{B} = \frac{1}{F} \quad (5)$$

This formula is correct for any Gaussian beam whose Rayleigh length $Z_R$ significantly smaller than |F-B| [3].

In this report the position of the virtual crossover (effectively the object) will be called A, the focal length of the magnetic lens will be called F, and B the position of the image.

The magnification relation that states that the ratio of the F length over the absolute value of F-B length is equal to the ratio of the B height $D_B$ over A height $D_A$. This is only true for a beam whose Rayleigh length $Z_R$ significantly smaller than |F-B| [3].

$$M = \frac{F}{|F-B|} = \frac{D_B}{D_A} \quad (6)$$

All lengths in this document are related to the center of the magnetic lens of the electron beam gun which is taken as 0.

The first part of this report reviews the effect of the main process parameters that the user is likely to change, beam current and lens current, on the caustic of the beam.

The second part aims to correlate the results obtained with the electron optics governing the system.

## Experimental

The welding machine of interest is the Pro-beam K25 electron beam welder equipped with a 500 mA 80 kV gun that can be used at accelerating voltages between 60 kV and 80 kV. The beam produced by a triode is focused on the work piece by a magnetic coil.

The emitting source is a 0.5 mm thick, 3 x 3 mm square tungsten electrode that is positioned into the cathode holder using the Pro-beam precision mounting equipment. The distance between the cathode and the magnetic lens is 611 mm.

The gun is placed at the top of the vacuum chamber facing down. The accelerating voltage throughout all measurements was 60 kV. All

measurements were done at vacuum levels of $10^{-4}$ mbar for the chamber and $10^{-5}$ mbar for the gun.

The aixACCT beam profiler (Fig. 1) consisting of a water-cooled pinhole faraday cup, which can operate at powers of up to 30 kW, was used to probe the beam. The faraday cup is mounted on a stage that can move vertically through a range of 150mm.This is a very important feature since it allows the real caustics of the beam to be determined. A magnetic deflection coil deflects the beam over the pinhole at a speed between 0 and 900 m/s.

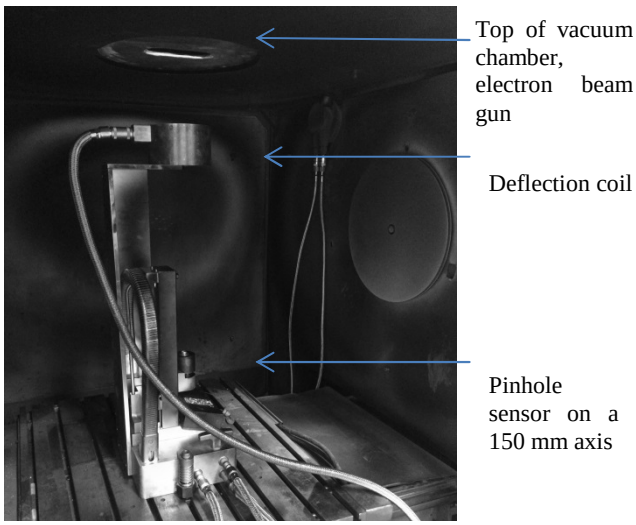


*Fig. 1. Experimental setup. AixACCT beam analyser*

The chamber of the K25 cannot accommodate a vertical movement of the beam analyser so the measurements were taken using only the 150 mm range of the beam analyser.

The beam analyser was used with a step height of 5 mm and the electron beam magnetic lens was used with steps of 5 mA. Therefore, the experimental errors are within ± 5 mm and ± 5 mA.

In this report, the beam diameter definition used is the canonical definition:

For a rotationally symmetric beam, the diameter $d_x$ is the diameter of a circle whose area $A_x$ encompass all amplitude values that are x % and superior to the maximum value.

$$d_x = 2\sqrt{\frac{A_x}{\Pi}} \quad (7)$$

The $d_{50}$ can be considered as the full width at half maximum (FWHM) whereas $d_{10}$ can be considered as the full width at $1/e^2$ (FWe2) which are naming more used and discussed in other papers.

Diabeam is the software provided with the beam analyser. Fig. 2 shows a beam caustic as obtained using the diabeam data.

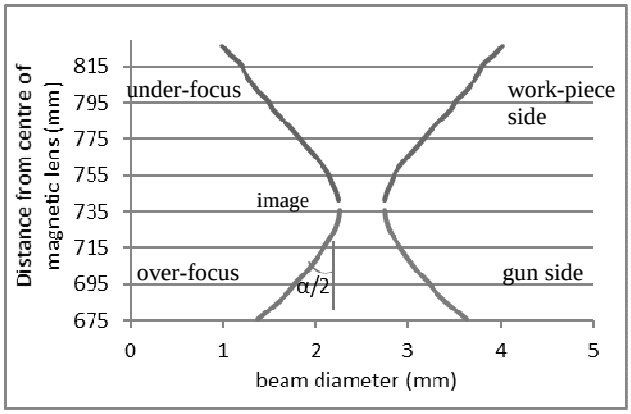


*Fig. 2. Caustic representation of the beam (using d10) as obtained by diabeam for a rotationally symmetric beam, upper part: over-focus, bottom part under-focus. Here 20 mA beam at 1.825 A lens current.*

For clarity, all lens current values $I_L$ will be expressed in Ampere (A) and all beam current values Ib will be expressed in milliAmperes (mA)

### *2.1. Effect of the lens current*

The effect of changing lens current on the beam position diameter and divergence is discussed in this part.

Beam currents ranging from 20 to 100 mA with increment of 20 mA were analyzed at lens currents ranging from 1.78 mA to 1.825 A at 5 mA steps.

Full caustics of the 20 mA set was recorded whereas for the 40, 60, 80 and 100 mA only the focal position and beam diameter values were recorded.

The filament was heated to temperature using the pro-beam automatic software. The beam analyser deflection speed was setup based on the authors' experience at speed in m/s = 5*Beam_current in mA. For example, for a 100 mA beam, the deflection speed is 500 m $s^{-1}$.

The equipment was not properly calibrated prior the 60 mA experiment, rendering the data not usable. As such, it is not presented.

### *2.2. Effect of beam current*

The effect of changing beam current on the beam position, diameter and divergence is discussed in this part.

Beam currents ranging from 10 to 120 mA with increments of 10 mA were analysed at a constant lens current of 1.78 A and 1.825 A. The filament was heated to temperature as previously discussed and the beam analyser deflection speeds were chosen as per 0.

The focus position at the 1.825 A data set was close to the top of the beam analyser's range therefore no divergence could be calculated.

### *2.3. Crossover properties*

The pro-beam equipment comes with a formula stating the value of the focal length of the gun's magnetic lens as a function of the lens current.

$$F = \frac{19.356 * V}{I_L^2} \quad (8)$$

Where F is the focal length in mm, V the accelerating voltage in kV and $I_L$ the lens current in Amp. This formula does not include the relativistic compensation but will nevertheless be used as is.

The values from section 3.2 will be used to quantify the virtual crossover position and diameter This data will then be used to create a mapping of the electron beam source and allow the results to be compared to the curves obtained in 3.1.

## Results and discussion

### *3.1. Effect of lens current*

Fig. *3* shows that increasing the lens current, reduces the working distance required to maintain focus. This is due to the lens' focal length being inversely proportional to the lens current as per (3).

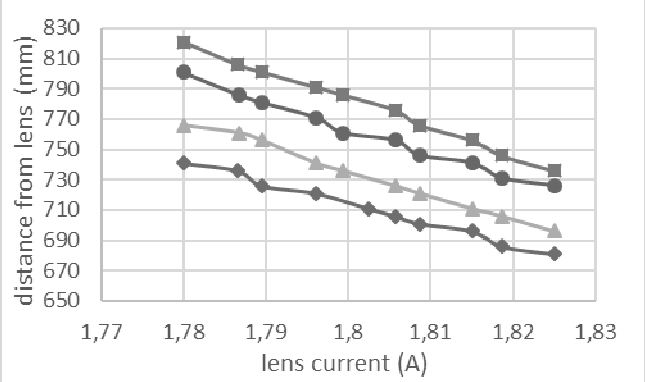


*Fig. 3. Effect of lens current on the distance to lens' center as a function of the lens current, square Ib 20 mA, circle Ib 40 mA,triangle Ib 80 mA, diamond Ib 100 mA*

Fig. 4 shows the effect of lens current on the beam diameter. The curves show that increasing the lens current increases the beam diameter. It is also evident that at higher beam current, the beam diameter increases.

Fig. 5 shows the half divergence angle of the 20 mA beam as a function of the lens current. It is seen that the divergence angle in the upper part of the beam, called overfocus, reduces with lens current and the part past the image, called underfocus, increases with lens current. The curve also shows that there is a lens current for which, the divergence angle on both sides of the image is equal. Not shown but observed by the authors is that at higher lens currents, the two curves cross so that the over-focus divergence angle gets smaller than the under-focus one.

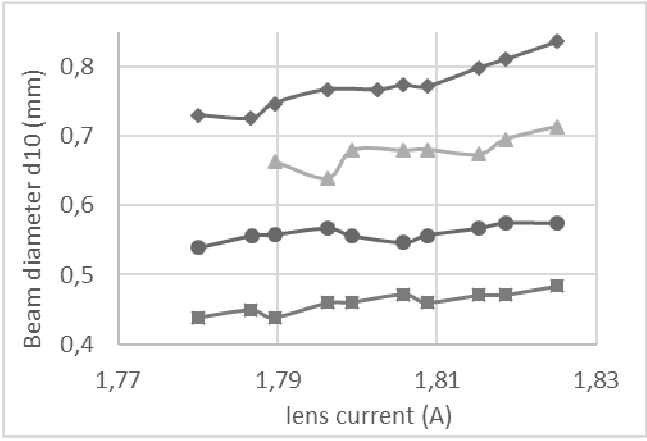


*Fig. 4. Variation of beam size d10 as a function of lens current, square Ib 20 mA, circle Ib 40 mA,triangle Ib 80 mA, diamond Ib 100 mA*

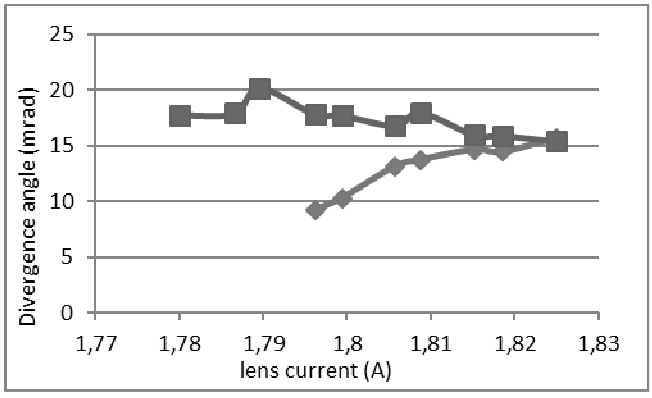


*Fig. 5. Half divergence angle as a function of lens current for the 20 mA beam, square over-focus angle, diamond under-focus angle.*

The emittance was calculated using equation (1). The results can be seen in Fig. 6.

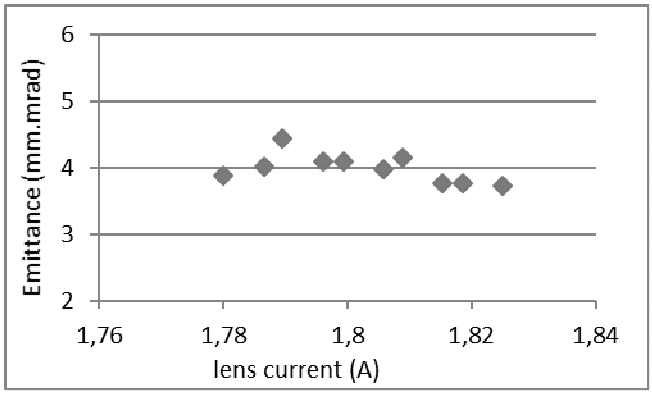


*Fig. 6. Variation of emittance as a function of lens current*

The emittance remains constant with varying lens current. This illustrates clearly the conservation of the emittance and agrees with Liouville's theorem. This emittance value describes not only the emittance of the image but also the emittance of the crossover.

### *3.2. Effect of beam current*

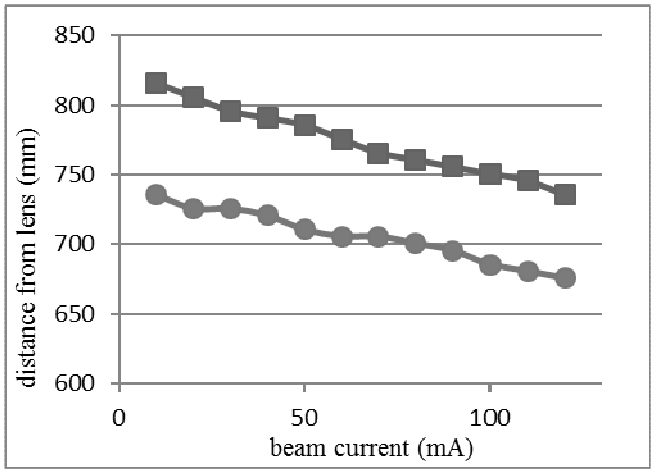


*Fig. 7. Shifting of the image as a function of power at constant lens current, square IL 1.78 A, circle IL 1.825 A*

Fig. 7 shows that at a constant lens current, between 10 and 120 mA, there is a regular shift of the image towards the magnetic lens; this is what is regularly referred to as focus-shifting.

The gradient of the curve represents the rate at which the focus position changes with respect to the beam current. From the data shown in Fig. 7 it can been seen that at higher lens currents this rate of change is lower than it is at lower lens currents. Therefore, one can speculate that the focus shifting is less significant at higher lens current than at lower lens current.

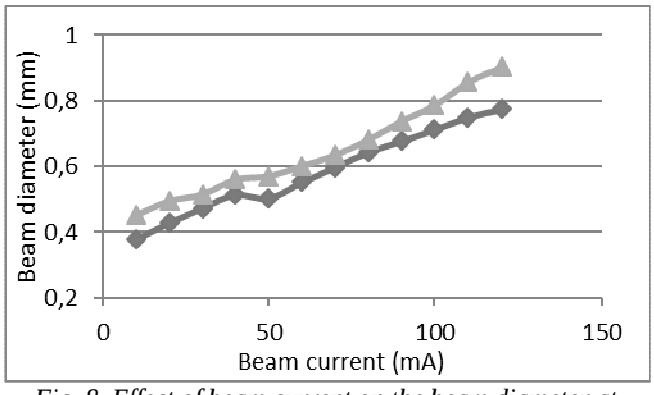


*Fig. 8. Effect of beam current on the beam diameter at image, diamond 1,78 A d10, triangle 1,825 A d10*

It can be seen in Fig. 8 that the diameter d10 increase with increasing beam current. This is due to the larger amount of electrons in the beam and hence stronger space charge effect.

The same effect explains why the more focused beam at 1.825 A lens current is wider than the less focused one at 1.78 A.

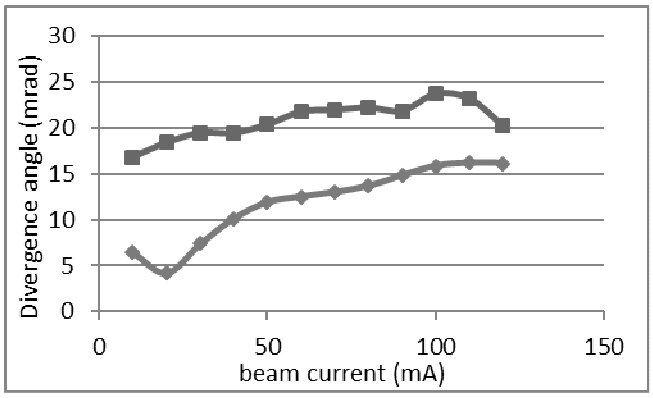


*Fig. 9. Effect of the beam current on the half divergence.square over-focus, diamond under-focus, at IL 1.780 A*

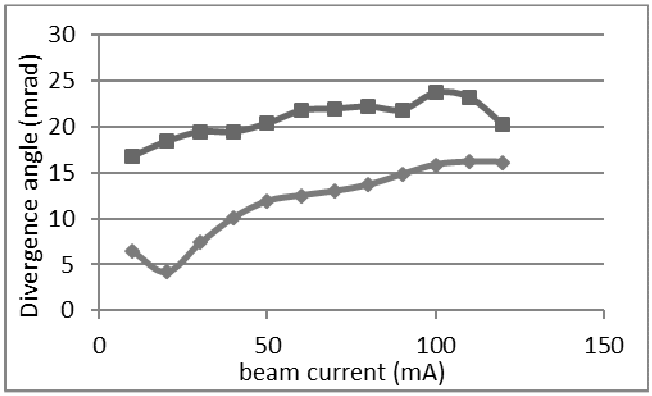


Fig. *9* shows that the beam divergence, both in the over-focus and under-focus parts of the beam increase with higher beam currents. This is directly related to the space charge effect.

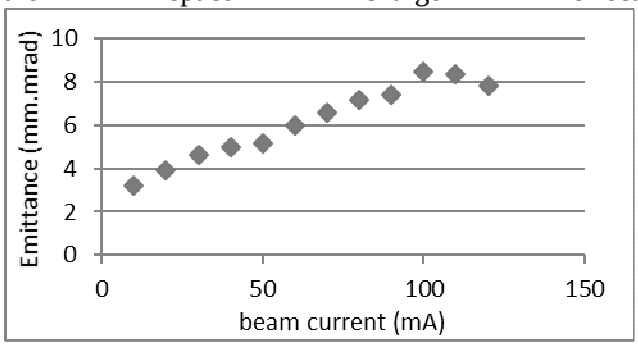


Fig. *10* displays the influence of beam current on emittance.

In a Gaussian beam, the Rayleigh length is the distance from lowest beam diameter $d_{min}$ such that $d(Z_R)= \sqrt{2}\, d_{min}$ [3].

In the case of the 20 mA beam, the beam with lowest divergence, the Rayleigh length is 24 mm (if

one only accounts for the divergence on the side of the magnetic lens).

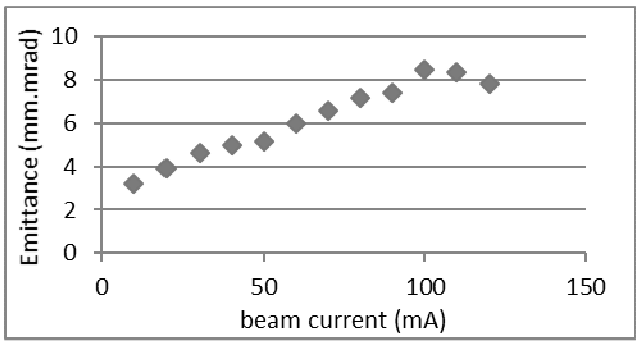


*Fig. 10: Emittance as a function of beam current at IL 1.78 A lens current*

The emittance increases with beam current. The higher beam current, and thus spatial charging, cause an increase in the beam diameter leading to an increase in emittance.

### *3.3. Crossover properties*

#### *3.3.1. Crossover position*

Some magnetic lenses behave as thin lenses and nothing let the authors suppose that the magnetic lens of the gun to be a thick or asymmetric lens [5] especially since only one value of focal length was given by the manufacturer. Also the Rayleigh length of the beam between 20 and 100 mA is shown to be very small compared to the distance between F and B. As a consequence, the optical thin lens formula (5) was used on the data of the image B presented in Fig. 3 and using the values of F as per (8) to find the position of the virtual crossover A as:

$$A = \left(\frac{1}{F} - \frac{1}{B}\right)^{-1} = \frac{19.356 * V}{B * I_L^2 - 19.356 * V} \quad (9)$$

Fig. 11 shows the result for the position of the virtual crossover A.

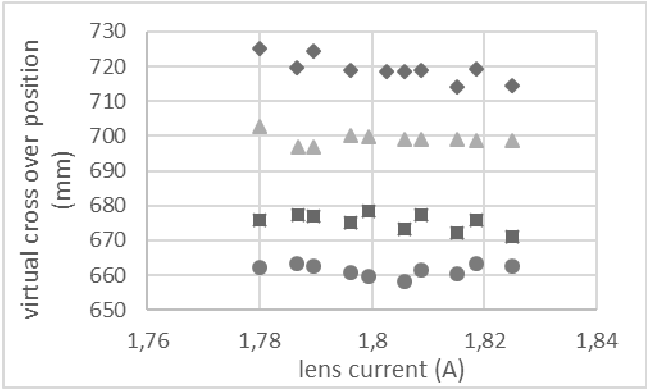


*Fig. 11. Position of the virtual crossover as a function of the lens current square Ib 20 mA, circle Ib 40 mA, triangle Ib 80 mA, diamond Ib 100 mA*

The virtual crossover position stays constant regardless of the lens current. This proves that the thin lens formula is indeed working for this gun's lens. The position does however vary with the beam current as shown.

The values of the virtual crossover position obtained correspond to a point beyond the cathode in the gun, which is a good indication that these results make sense. Indeed the virtual crossover cannot be further down the gun that the real crossover.

The same equation (9) was used on the data presented in Fig. 7 to observe the evolution of the virtual crossover with beam current. Fig. 12 shows the results.

The values obtained for the virtual crossover positions for the two sets of data should be equal as proven in Fig. 11. They are quite similar with a maximum error of 10 mm between the two sets. This is actually within the experimental error of the experiment.

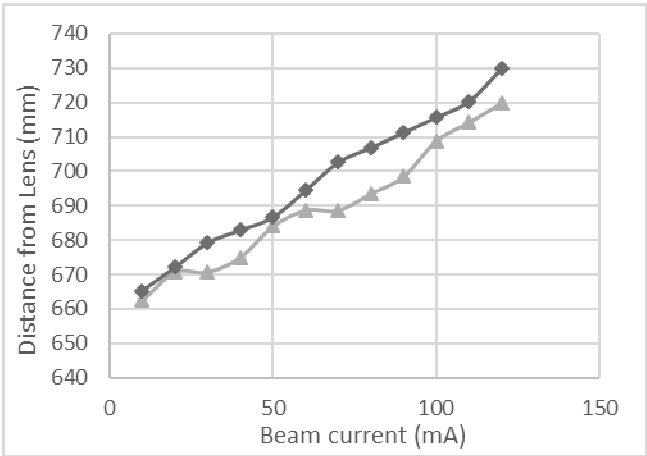


*Fig. 12. Position of virtual crossover as a function of beam current, triangle virtual crossover 1.825 A, and diamond virtual crossover 1.78 A*

### 3.3.2. Crossover diameter

Using the magnification equation (6) on the beam diameters of Fig. 4 we obtain the beam diameter of the virtual crossover.

The results are shown in Fig. 13.

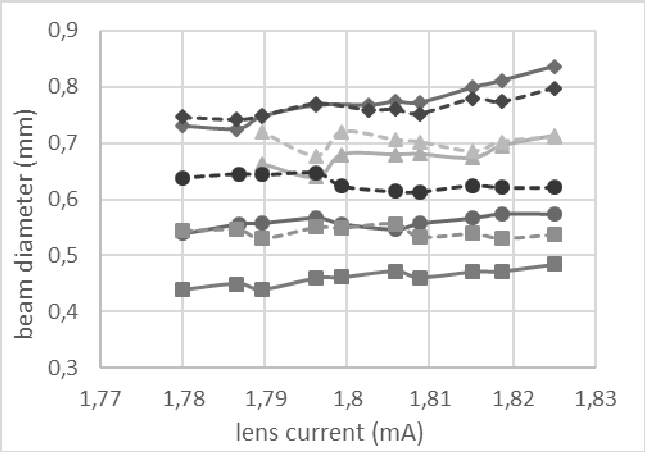


*Fig. 13. Diameter of the virtual crossover d10 as a function of lens current (dashed line) and comparison with beam diameter d10 at image (solid line) square, Ib 20 mA, circle, Ib 40 mA, triangle Ib 80 mA, diamond Ib 100 mA.*

The diameter of the crossover is displayed. It can be considered constant as function of the lens current.

One can see for the case of the 20 mA and 40 mA beam that the magnification is inferior to 1. Hence a larger beam at the crossover than at the image itself.

For the 80 and 100 mA beam currents, it can be seen that the diameter of the virtual crossover is the same as the diameter of the image. In optics, this is a known phenomenon where the position of the object is exactly at twice the focal length of the lens. Using (5), this also means that the position of the image is at twice the focal length of the lens. This results in having a magnification equal to 1. Here, this is the case with the focal length being roughly 350 mm and the virtual crossover being around 700 mm from the centre of the lens.

Equation (6) was used on the data of Fig. **8** to assess the evolution of the virtual crossover diameter. Results are shown in Fig. 14.

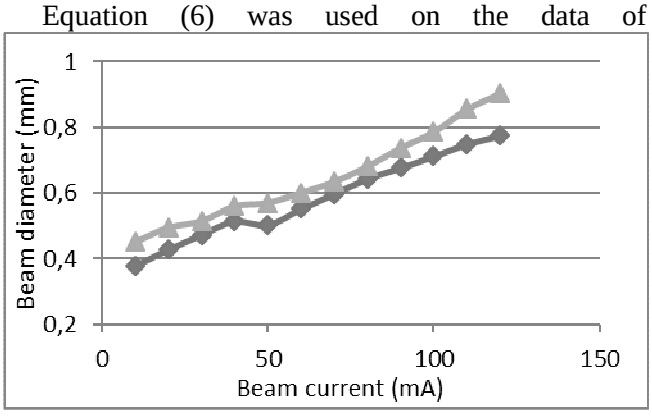


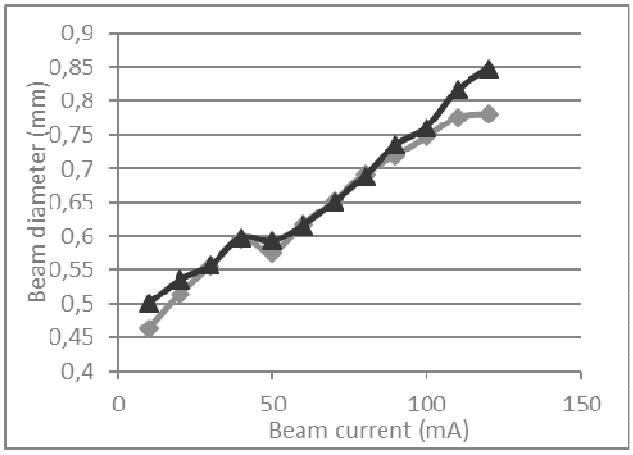


*Fig. 14. Evolution of the virtual crossover diameter as a function of beam current, triangle IL 1.78 A, diamond IL 1.825 mA*

It can be seen once again, that the beam diameters achieved for the virtual crossover are very similar. The virtual crossover diameter also increases with beam current.

### 3.3.3. Generalisation

The position, diameter and emittance of the virtual crossover were determined using 3.3.1, 3.3.2 and 3.2 respectively.

If one now uses the set of virtual cross over position values obtained in Fig. 12, and feed them in equation (10) one is able to determine the position and of the beam for all lens currents.

$$B = \left(\frac{1}{F} - \frac{1}{A}\right)^{-1} = \frac{19.356 * V}{A * I_L^2 - 19.356 * V} \quad (10)$$

Fig. 15 shows the comparison between the curves of the image B obtained using the virtual crossover object A values and the points of B obtained by beam analysis in Fig. 3.

There is good agreement between the curves obtained and the measured curves by beam analysis with each measured curve being closely related to the corresponding calculated curve. This is however limited by the experimental error of these two experiments.

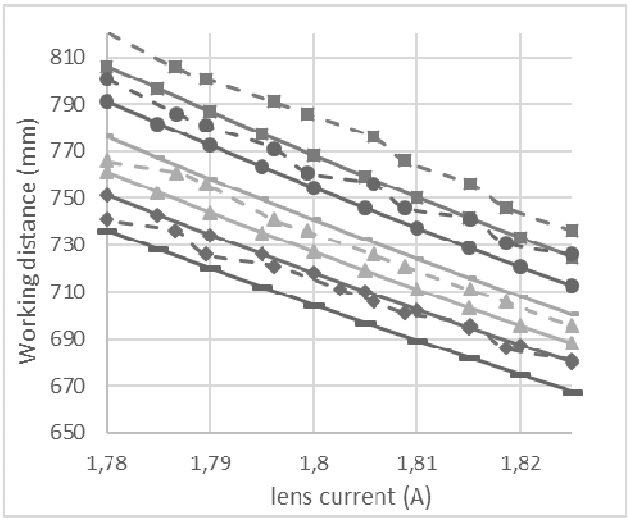


*Fig. 15. Comparison between the curves obtained in Figure 1 (dashed line) and the position of B calculated using the virtual crossover obtained in Fig. 12 (solid line). square Ib 20 mA, circle Ib 40 mA, bar 60 mA, triangle Ib 80 mA, diamond Ib 100 mA, long bars 120 mA.*

Fig. 16 shows the curves over the full lens operating range. For clarity, only the 10 mA, 60 mA and 120 mA curves are shown.

The influence of the magnetic focusing is not constant. At low lens currents, the image moves significantly as a function but this effect diminishes as the lens current is increased. Concerning focus shifting, it is minimum at high lens current, but is significant at low lens current. This agrees with the remark made for Fig. 7.

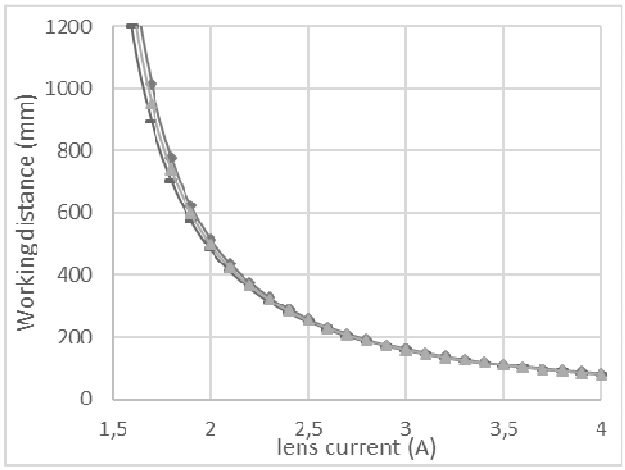


*Fig. 16. Distance from magnetic lens as a function of lens current, bars 120 mA, triangle 60 mA diamonds 10 mA*

The beam diameter can be calculated using equations (5) and (6) and the values for the virtual crossover diameter obtained in Fig. 14. The results compared with the beam diameter values observed in 3 are shown in Fig. 17.

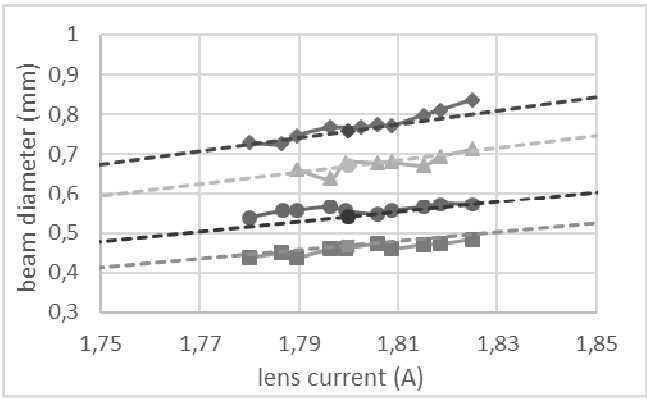


*Fig. 17. Comparison between the beam diameter obtained in Figure 3 (solid line) and the beam diameter calculated using the virtual crossover diameter obtained in Fig. 14 (dashed lines). square Ib 20 mA, circle Ib 40 mA, bar Ib 60 mA, triangle Ib 80 mA, diamond Ib 100 mA.*

Once again, there is clear agreement between the two different set of data. The beam diameter is clearly shown to increase as a function of lens current and beam current. Fig. 18 shows the curves over the full lens operating range. For clarity, only the 10 mA, 60 mA and 120 mA curves are shown.

At low lens currents, the beam diameter varies slowly with lens current, but as the lens current is increased, the beam diameter increase significantly.

If one defines the beam diameter-shift as the diameter evolution of the beam as a function of beam current, it can be seen that at high lens current, the beam diameter shift is more important that at low lens current.

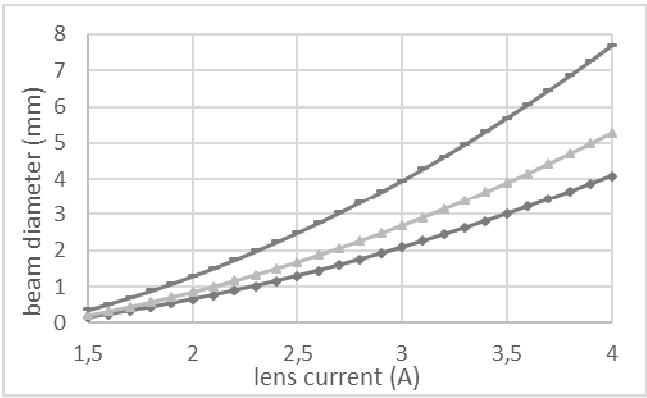


*Fig. 18. Beam diameter as a function of lens current, bars Ib 120 mA, triangle Ib 60 mA diamonds Ib 10 mA*

Through the conservation of emittance (1), one can determine the divergence of the beam in the overfocus side. For clarity, only the 10 mA, 60 mA and 120 mA curves are shown.

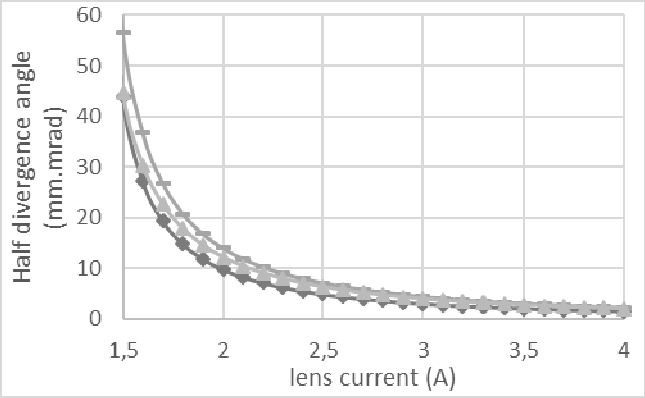


*Fig. 19. Half divergence angle of the beam as a function of lens current, bars Ib 120 mA, triangle Ib 60 mA diamonds Ib 10 mA.*

As observed by beam analysis, the divergence angle diminishes with the lens current and increases with the beam current.

**Conclusions**

- The beam analyser as well as electron optics formulas allow to determine the position, diameter and divergence of the virtual cross over at each beam current.
- This can then be used to obtain the position, diameter and divergence of the image through a lens of known characteristics.
- Achieving a mapping of one's electron source as a function of input parameters is the way forward that electron beam users should achieve to improve the transferability between different equipment.
- It is now a matter of understanding and quantifying the influence of other parameters such as cathode ageing, poor filament heating, poor filament placing, and vacuum levels that also have an effect on the position and diameter of the beam.

**Acknowledgements**

The authors wish to thank the High Value Manufacturing Catapult for sponsoring this project.

**REFERENCES**

[1] P. W. Hawkes, E. Kasper. Principles of Electron Optics. 1996, ISBN: 978-0-12-333340-7

[2] H. Schultz. Electron beam welding. Cambridge, Abington-publishing, 1994, pp. 11, ISBN 3-87155-111-2

[3] S. A. Self. Focusing of spherical Gaussian beams. Applied optics, 1983, pp. 658-661

[4] A. B. El-Kareh. Electron beams, lenses, and optics. Volume 1, 1970, pp. 253-307, ISBN: 978-0-12-238001-3

[5] P. W. Hawkes. Magnetic electron lenses. Springer-verlag, 1982, pp. 125, ISBN: 978-3-642-81518-8

***Electron Beam Welding Engineer, Thomas Dutilleul*** *- Was born in Wattrelos, France 1990. He holds a MSc in Welding Engineering from Cranfield University and a Master's degree in Physics from Lille University with specialisation in materials for nuclear applications. He is currently working at the Nuclear AMRC of the University of Sheffield, UK. His research interests are Electron Beam Welding and additive manufacturing.*

*e-mail: thomas.dutilleul@namrc.co.uk*

***Intern Electron Beam Welding Engineer, Joshua Priest*** *– Was born in Sheffield, UK 1995. He is studying MEng Mechanical Engineering at Sheffield Hallam University. He is currently on a placement year at the Nuclear AMRC of the University of Sheffield, UK. His research interests are Electron Beam Welding and additive manufacturing.*

*e-mail: joshua.priest@narmc.co.uk*

***Power Beam Technology Lead, PhD Bernd Baufeld****– Was born in Würzburg, Germany, 1964. He received his Ph.D. degrees in Physics at the Martin Luther Universtity Halle Wittenberg, Germany 1996. Author of 98 scientific publications, 1 patent. He is currently working at the Nuclear AMRC of the University of Sheffield, UK. His research interests are Electron Beam Welding, Laser Welding and Cladding and additive manufacturing.*

*Tel.:+44 (0) 114 222 9919;*

*e-mail: b.baufeld@namrc.co.uk*